Ascorbyl-dipalmitate-stabilised nanoemulsions as a potential localised treatment of inflammatory bowel diseases

M. Plaza-Oliver [a, b], A. Beloqui [c], M.J. Santander-Ortega [a, b], L. Castro-Vázquez [a, b], V. Rodríguez-Robledo [a, b], M.M. Arroyo-Jiménez [a, b], V. Préat [c, #]. M.V. Lozano [a, b, #].

[a] Cellular Neurobiology and Molecular Chemistry of the Central Nervous System Group, Faculty of Pharmacy.

[b] Regional Centre of Biomedical Research (CRIB). University of Castilla-La Mancha (UCLM), Albacete 02008, Spain.

[c] Université Catholique de Louvain, Louvain Drug Research Institute, Advanced Drug Delivery and Biomaterials, Brussels, 1200, Belgium.

Corresponding authors

Email: veronique.preat@uclouvain.be. Phone: +32 27647320 (V.P.)

Email: mvictoria.lozano@uclm.es. Phone: +34 967599200 ext. 8238 (M.V.L.)

Abstract

Current efforts on inflammatory bowel diseases (IBD) treatment are focused on strategies for localised drug delivery at the intestinal mucosa. Despite the potential of curcumin (CC) for IBD treatment, its low solubility and stability limit its application. Thus, the design of nanocarriers that focus CC delivery at the intestinal epithelium is an area of interest. This work proposes α-tocopherol nanoemulsions (NE) stabilised by ascorbyl-2,6-dipalmitate (ADP) as intestinal CC-carriers. The antioxidant capacity of α-tocopherol and ADP could have a synergistic effect on IBD-affected tissues, characterised by an oxidative environment. We obtained nanoemulsions (NE-ADP) with size below 200 nm, negative surface charge,

stable in gastrointestinal media and no toxic in the Caco-2 cell model. Intracellular retention of NE-ADP in Caco-2 cells was observed by confocal microscopy. The extremely low P_{app} values obtained for CC and α-tocopherol indicated the lack of transport across the Caco-2 monolayer. Control nanoemulsion stabilised by lecithin (NE-L) was greatly transported across the Caco-2 cells monolayer, confirming the relevance of ADP on the cellular retention of NE-ADP. The therapeutic potential of NE-ADP was shown by the significant decrease of intracellular ROS levels. Altogether, these results indicate the potential of NE-ADP as a novel approach for the treatment of IBD.

Keywords

Ascorbyl-2-6-dipalmitate

Nanoemulsion

Curcumin

IBD

Antioxidant

Localised Drug Delivery

Abbreviations

ADP: Ascorbyl 2,6-dipalmitate

CC: Curcumin

CC-loaded NE-L: curcumin loaded nanoemulsions stabilised by lecithin

CC-loaded NE-ADP: curcumin loaded nanoemulsions stabilised by ascorbyl dipalmitate

DCFDA: Dichlorofluorescein diacetate

DCFH-DA: Oxidised derivative of dichlorofluorescein diacetate

GI: Gastrointestinal

IBD: Inflammatory Bowel Diseases

NE: Nanoemulsion

NE-ADP: Nanoemulsions stabilised by ascorbyl dipalmitate

NE-L: Nanoemulsions stabilised by lecithin

SGF: Simulated Gastric Fluid

SIF: Simulated Intestinal Fluid

1. Introduction

The term inflammatory bowel diseases (IBD) groups several chronic inflammatory disorders of the gastrointestinal (GI) tract, including Chron's disease and ulcerative colitis, whose incidence is increasingly growing worldwide. IBD is an intermittent disease, based on flares and remissions. During flares, the most common symptoms include diarrhoea, abdominal distension and pain, nauseas, vomiting, fever and rectal bleeding (Bernstein et al., 2010; Prantera, 2013). Furthermore, IBD can lead to more severe complications, such as toxic megacolon, colon cancer, or bowel perforation, among others (Bernstein et al., 2010). Although the pathogenesis of IBD is not completely understood, genetic factors and altered intestinal microbiota may be involved in the onset of the intestinal immune response dysregulation, what finally causes intestinal injury (Bernstein et al., 2010; Hvas et al., 2018). In addition, there is strong evidence suggesting that ROS-induced oxidative stress also plays a relevant role in IBD pathogenesis and progression (Guan and Lan, 2018; Kruidenier et al., 2003; Tian et al., 2017).

The current therapeutic strategies aim to relief flare-symptoms and avoid hospitalisation or surgery. In this sense, a long-term treatment based on a combination of drugs is often needed to control the disease. More concretely, the therapeutic approach includes anti-inflammatory drugs (aminosalicylates and systemic glucocorticoids), biological agents (such as anti-TNF-α monoclonal antibodies), immunosuppressive molecules and antibiotics (Hvas et al., 2018). Nonetheless, most of these treatments involve relevant unwanted side effects, mainly related to their systemic administration (Rogler, 2010; Stallmach et al., 2010). In this sense, localised drug delivery systems to the damaged mucosa would enhance the therapeutic potential and the safety of the treatments (Grimpen and Pavli, 2010; Siew et al., 2004).

Currently, the administration of antioxidant and anti-inflammatory natural molecules is a strategy under research (Bitiren et al., 2010; Hanai et al., 2006; Sugimoto et al., 2002; Tian

et al., 2017). More specifically, curcumin (CC) has recently attracted attention for its encouraging *in vivo* results in reducing both oxidative damage and inflammation at the GI tract (Arafa et al., 2009; Burge et al., 2019; Hanai et al., 2006; Sugimoto et al., 2002). In fact, CC is a potent inhibitor of NF-κB, cycloxygenase-2 and STAT3 pathways (Burge et al., 2019; Du et al., 2014; Hanai et al., 2006). Nevertheless, CC poor water-solubility and stability at neutral and alkaline pH values greatly limit its therapeutic use (Anand et al., 2007). The development of CC-loaded nanocarriers is a promising approach for IBD (Beloqui et al., 2016, 2014; Sharma et al., 2019), as nanocarriers may improve drug solubility and stability but also promote the interaction with the intestinal epithelium (Plapied et al., 2011; Zhang et al., 2013). In this line, Beloqui *et al*. evaluated different lipid-based nanocarriers containing CC for IBD treatment. Interestingly, they observed that nanocarriers which were able to achieve CC retention at the GI tract were more efficient in treating IBD in a murine DSS-colitis model compared to those that enhanced CC intestinal permeation (Beloqui et al., 2016). These results highlighted the relevance of the nanocarrier structure and composition on the biological behaviour of the systems. Indeed, the functionalisation of nanocarriers with specific molecules is a strategy followed for potentiating their interaction with specific cell populations (Xu et al., 2020; Yoo et al., 2019). In this sense, enterocytes include different transporters and receptors that mediate their functionality, such as the sodium-dependent ascorbic acid transporter SVCT1. This transporter is involved in the maintenance of the ascorbic acid homeostasis in the organism (May, 2011). Since it is expressed at the apical brush of enterocytes, it has been recently proposed as a novel intestinal target (Luo et al., 2018).

The aim of this work was to formulate a nanocarrier able to improve CC solubility and deliver the drug to the intestinal mucosa site. We have recently reported the development of a new antioxidant nanoemulsion as a novel nanocarrier for oral delivery (Plaza-Oliver et al., 2020). This system, named as NE-ADP, is constituted by α-tocopherol which is a lipophilic antioxidant able to scavenge free radicals in hydrophobic environments (Kontush

et al., 1996). The core is stabilised by ascorbyl-2,6-dipalmitate (ADP) that maintains the antioxidant properties of ascorbic acid (Moribe et al., 2010). Hence, we proposed this two-component formula that would simultaneously act as a CC carrier and an antioxidant to the intestinal barrier. This dual-action was evaluated by studying the internalisation capacity of the systems and their ROS scavenging capacity in the enterocyte-like model in order to determine the potential of NE-ADP for the localised treatment of IBD. The involvement of SVCT1 in the uptake was qualitatively assessed by using an excess of ascorbic acid to saturate the transporter in order to preliminary determine the effectiveness of this surfactant targeted approach.

2. Materials and methods

2.1 Materials

2.1.1 Chemicals

Lecithin (Epikuron 145V) was kindly donated by Cargill (Spain). Poloxamer 127 (PF127®), α-tocopherol, CC, bovine serum albumin (BSA), dimethyl sulphoxide (DMSO), HEPES, MES hydrate, triton-X 100, dichlorofluorescein diacetate (DCFDA) and ascorbic acid were purchased from Sigma-Aldrich (Spain and USA, respectively). ADP was obtained from Combi-blocks (USA). Acetone, methanol, ethanol, 2-propanol and acetonitrile, HPLC grade, were acquired from VWR Chemicals (Belgium). ThermoFischer supplied 99 % glacial acetic acid. DiD [DiIC18(5) oil (1,1′dioctadecyl-3,3,3′,3′-tetramethylindodicarbocyanine perchlorate)] and rhodamin-phalloidin fluorescent tracers were purchased from Invitrogen (UK).

2.1.2 Cell culture reagents

Caco-2 cells (clone 1) were kindly donated by Dr Maria Rescigno, University of Milano-Bicocca (Milano, Italy) (Rescigno et al., 2001). Dulbecco's Modified Eagle Minimal Essential Medium (DMEM), fetal bovine serum (FBS) heat-inactivated HyClone, penicillin-

streptomicin (PEST), Hanks Balanced Salt Solution (HBSS), phosphate buffer saline (PBS), trypsin-EDTA (0.05 %) and non-essential aminoacids (NEAA) were purchased from Gibco™ (Invitrogen, UK). Basement membrane matrix (Matrigel®) was obtained from BD Bioscience (Belgium).

2.2 Nanoemulsions formulation

Nanoemulsions of α-tocopherol were formulated following the solvent displacement technique, which briefly consists on the spontaneous emulsification of an oily phase into 10 mL of ultrapure water under magnetic stirring. We followed a procedure previously described with slight modifications (Lozano et al., 2013; Plaza-Oliver et al., 2020). The organic phase was a solution of α-tocopherol (38 mg) and lecithin (20 mg) in 250 μL of ethanol and 4.75 mL of acetone to yield NE-L systems. The organic phase for the NE-ADP formulations was obtained by dissolving α-tocopherol (38 mg) and ADP in 5 mL of acetone. Two different NE-ADP were obtained: NE1-ADP (9 mg ADP) and NE2-ADP (17 mg ADP). In all cases, organic solvents were eliminated to a final volume of 4 mL and the nanoemulsions were further incubated for 24 h with 1 mL of a PF127® aqueous solution (3 mg/mL) to allow the adsorption of the surfactant to the surface of the nanoemulsions. This PF127® ratio per batch (3 mg) was selected after the evaluation of different PF127® amounts in the range 1.5-12.5 mg for obtaining the coated nanoemulsions.

CC was then encapsulated in the inner core of the nanoemulsions. For this purpose, we followed the same formulation procedure but adding 200 μL of an ethanolic CC solution (2.5 mg/mL) to the oily phase. This way, the CC loading was 0.8 % for NE-L, 1 % for NE1-ADP and 0.9 % for NE2-ADP.

Fluorescence labelling of the nanoemulsions was carried out by the incorporation of the lipophilic tracer DiD (λ_{ex}≈644nm, λ_{em}≈665nm) to their oily phase during the formulation process. Briefly, 40 μL of a methanolic DiD solution (6.25 mg/mL) were mixed with the rest of the organic components. After obtaining the labelled nanoemulsions, they were dialysed

(10,000 MWCO) for 24 h, in order to remove the non-encapsulated DiD. Then, they were incubated with 1 mL of a PF127® aqueous solution (3 mg/mL) for 24 h, yielding to a final DiD concentration of 8 µL/mL.

2.3 Physicochemical characterisation and colloidal stability

The determination of the hydrodynamic mean diameter, polydispersity index and δ-potential was carried out by dynamic light scattering (DLS) and measurement of the electrophoretic mobility, using a NanoZS from Malvern (UK). For this purpose, nanoemulsions were previously dispersed (5 µL/mL) in phosphate buffer 2 mM.

The long-term stability of the nanoemulsions was evaluated at 4 °C for one month. Stability of the systems in plain (not enzymes-enriched) and normal simulated gastric and intestinal fluids (SGF and SIF, respectively) following the USP (XXIX) guidelines for 4 h at 37 °C was also studied. Similarly, it was necessary to assess the stability of the nanoemulsions under the conditions of *in vitro* experiments. For that purpose, nanoemulsions were incubated with growth (DMEM) and transport (HBSS) media for 2 h at 37 °C.

2.4 CC encapsulation efficiency and release in transport media

The encapsulation efficiency (EE) of CC in CC-loaded nanoemulsions was assessed by isolating the unloaded CC using ultrafiltration and determining the amount of CC in the filtrate. Briefly, nanoemulsions were placed at the top of centrifuge filtration tubes (100,000 MWCO, Amicon®) and centrifuged at 1,500 rcf for 20 min. As a result, a transparent filtrate was obtained at the bottom of the tubes, whereas nanoemulsions remained intact at the upper part of the device. The diffusion of unloaded CC across the filter was confirmed by the ultrafiltration of a CC solution and the determination of the drug concentration in the filtrate. The quantification of CC was performed by HPLC and the EE values were indirectly calculated by the following equation:

$$EE = (100\ x\ (C_0 - C))/C_0 \qquad \textbf{Eq. 1}$$

where C_0 refers to the theoretical encapsulated CC concentration and C to its concentration in the filtrate.

A similar procedure was carried out for the determination of CC released into transport media (3 mM MES HBSS, pH 6.5). For that purpose, nanoemulsions were first incubated with this media for 2 h at 37 °C. Then, they were placed at the top of centrifuge filtration tubes (100,000 MWCO) and centrifuged at 1,500 rcf for 20 min. Finally, the CC present in the resulting filtrates was quantified by HPLC.

2.5 CC suspension preparation

CC suspension (CC-sus) was formulated by dispersing 10 mg of CC in 5 mL HBSS containing 3mM MES (pH 6.5). The control CC-sus was homogenised under sonication (60 sec) at a power of 60 W under magnetic stirring (1,000 rpm) and its particle size was measured by laser diffraction (HELOS, Sympatec, Clasthal-Zellerfeld, DE). The control was obtained by the dilution of CC-sus to a final concentration of 0.05 mg/mL.

2.6 CC and α-tocopherol quantification by HPLC

The quantification of both α-tocopherol and CC was carried out following procedures previously described with minor modifications (Beloqui et al., 2016, 2014; Cui et al., 2009; Memvanga et al., 2013; Villaseca-González et al., 2018). For this purpose, a Shimazu 20A Series HPLC system with a diode array detector, equipped with an EC 250/2 Nucleodur 100-5C18 column (250x4,6mm, particle size: 5.0 µm) (Macherey-Nagel, DE) was used. Regarding α-tocopherol, the mobile phase consisted on a 2-propanol: acetonitrile mixture (50:50 v/v). Samples were diluted in mobile phase before injecting (20 µL injection volume) and afterwards isocratically eluted at a 1 mL/min flow rate. The wavelength detection was set at 295 nm (Villaseca-González et al., 2018). The limits of detection (LOD) and quantification (LOQ) of α-tocopherol were 0.5 and 1.7 mg/mL. The mobile phase for CC determination consisted on a mixture of methanol and 3.6 % glacial acetic acid (73:27 v/v). The samples (50 µL injection volume) were diluted in the mobile phase and then isocratically eluted at a

0.8 mL/min flow rate (Beloqui et al., 2016, 2014; Cui et al., 2009; Memvanga et al., 2013). The wavelength detection for CC was set at 428 nm. Following this method, LOD and LOQ of CC were 5 ng/mL and 20 ng/mL, respectively.

2.7 In vitro studies in Caco-2 cells

2.7.1 Cell culture

Caco-2 cells were cultured in DMEM supplemented with 1 % (v/v) PEST, 1 % (v/v) NEAA, 1 % (v/v) L-glutamine and 10 % (v/v) heat-inactivated FBS in 175 cm^2 flasks (Corning, MA, USA) under an atmosphere of 10 % CO_2/ 90 % air at 37 °C. The culture media was replaced every 2 days, and regular passaging was performed by trypsinisation. Cells were used between passages x + 24 and x + 30.

2.7.2 Nanoemulsions effect on cell viability

The cytotoxicity of the nanoemulsions was assessed in Caco-2 cells by the crystal violet assay. Briefly, 2 x 10^4 cells/well were seeded in 96-well plates coated with Matrigel® and incubated at 37 °C for 24 h. Caco-2 cells were then exposed to both unloaded and CC-loaded nanoemulsions (NE-L, NE1-ADP and NE2-ADP) dispersed in 100 µL plain DMEM at increasing concentrations (2-90 %) (v/v). After 2 h, the supernatants were removed and 100 µL of a 0.5 % (w/v) crystal violet staining solution were added to each well. Next, Caco-2 cells were incubated at 37 °C for 30 min, washed twice with ultrapure water and air dried for 30 min. Finally, 100 µL of methanol were added to each well and 30 min later the optical density was measured at 570 nm with a plate reader (MultiSkan EX plate reader, ThermoFischer Scientific, MA, USA). Caco-2 cells treated with DMEM or with Triton-X 100 were considered as negative and positive controls, respectively.

2.7.3 Permeability studies of unloaded and CC-loaded nanoemulsions across Caco-2 cell monolayers

A Caco-2 cell monolayer was obtained following a protocol previously described (Beloqui et al., 2017, 2016, 2014). Briefly, Caco-2 cells were seeded in 12-well culture inserts (1 µm pore diameter, 0.9 cm^2 area, Corning Costar®, NY) at a density of 5 x 10^5 cells/well and grown for 21 days in supplemented DMEM by replacing media every other day. The integrity of the monolayers was evaluated by measuring the trans-epithelial electrical resistance (TEER) before and after the transport studies. These measurements were carried out at 37 °C using an epithelial voltmeter (EVOM, World Precission Instruments, Berlin, DE) that allowed us to select those monolayers with TEER values over 200 Ω/cm^2 for the experiments.

α-tocopherol was used as a marker of unloaded nanoemulsions permeability across Caco-2 cells monolayers. For that purpose, 500 µL of NE-L, NE1-ADP or NE2-ADP dispersed in HBSS were added to the apical side of the inserts at a concentration of 500 µL/mL which was previously shown to be safe in the cytotoxicity tests. The basolateral side of the inserts was then filled with 1 mL HBSS, and after 2 h at 37 °C and sampled for α-tocopherol quantification by HPLC.

Next, the apparent permeability coefficient (P_{app}, cm/s) was calculated for each formulation, according to the following equation:

$$P_{app} = dQ/dt \; x \, 1/AC_0 \qquad \textbf{Eq. 2}$$

Where dQ/dt refers to the transport rate (µg/s), A to the surface area of the membrane filter (cm^2) and C_0 to the initial α-tocopherol concentration in the apical side (µg/mL) (Beloqui et al., 2016, 2014).

Next, we assessed the permeability of CC-loaded nanoemulsions, compared to CC-sus, across Caco-2 cells monolayers. For this purpose, we included slight modifications to the procedure described previously e.g., the modification of the transport media to assure CC solubility and stability (Beloqui et al., 2016). Accordingly, 3 mM MES HBSS (pH 6.5) was

used for dispersing CC-loaded NE-L, CC-loaded NE-ADP or CC-sus at the apical compartment. The basolateral side was filled with 1 mL 10 mM HEPES HBSS + 1 % BSA (pH 7.4) (Beloqui et al., 2016, 2014). Finally, P_{app} values for CC were calculated following Eq. 2. In this case, C_0 refers to the initial CC concentration (50 μg/mL) at the apical side.

Additionally, we evaluated the amount of CC associated or intracellularly localised in Caco-2 cells. For this purpose, we pre-treated the Caco-2 monolayer to lysate the cells and enable the release of CC, by washing thrice the inserts with HBSS and filling them with 1 mL of sterile water. Then, we exposed Caco-2 cells to three freeze-thawing cycles in order to disrupt their membranes (Islam et al., 2017). Finally, cell lysates were centrifuged at 250 rcf at 4 °C for 5 min, and the supernatants were collected for CC quantification by HPLC.

2.7.4 Localisation of nanoemulsions in Caco-2 cell monolayers

The localisation of DiD-loaded nanoemulsions (NE-ADP and NE-L) in Caco-2 monolayers was performed by confocal laser scanning microscopy (CLSM). For this purpose, we followed the procedure described in section 2.7.3. This time, after the 2 h incubation, inserts were washed twice in warm PBS and then once in cold PBS. Afterwards, inserts were fixed in cold 4 % (v/v) paraformaldehyde (PFA) (500 μL/insert) for 30 min and gently washed in PBS. In order to reveal cell borders, actin was stained with 200 μL of rhodamin-phalloidin (1:100) in HBSS + 0.2 % (v/v) Triton X-100. Inserts were then incubated for 30 min in the dark, washed in PBS, cut and mounted on glass slides with Vectashield® mounting medium containing 4',6'- diamidino2-phenylindole (DAPI) 1:20 to stain cellular nuclei (Beloqui et al., 2016). Images were captured using a LSM710 confocal microscopy from ZEISS (Axio Imager Z.1) and analysed with the ZEN (black edition 2.1) software to obtain *x-y*, *x-z* and *y-z* views of the Caco-2 monolayers.

In order to evaluate the role of SVCT1 in the uptake of NE-L and NE-ADP, we also carried out this experiment after a previous incubation of the Caco-2 cell monolayers with the substrate of this transporter. 20 days after the seeding of Caco-2 cells in the inserts, we pre-

incubated them with an ascorbic acid solution (100 μM) at 37 °C for 24 h. After this time (day 21), TEER measurements were carried out to evaluate the effect of the pre-incubation with ascorbic acid on the integrity of the Caco-2 cells monolayers. Then, we incubated cells with the nanoemulsions for 2 h and we followed the experimental procedure above described to obtain images of the Caco-2 cells monolayers by CLSM.

2.7.5 Intracellular ROS levels measurements

The effect of the formulations on the intracellular ROS levels were evaluated by dichlorofluorescein assay, following a procedure previously described (Djiokeng Paka et al., 2016; Jiménez et al., 2016). In this experiment, Caco-2 cells were seeded at a density of 2 x 10^4 cells/well in 96 well plates coated with Matrigel™ and incubated for 24 h at 37 °C. Then, Caco-2 cells were incubated for 2 h with the different treatments, namely CC-sus, unloaded or CC-loaded NE-L and NE1-ADP, at a concentration corresponding to 3,800 μg/mL of α-tocopherol and 50 μg/mL of CC. Additionally, H_2O_2 0.3 % (v/v) and PBS were used as positive and negative controls, respectively. Next, cells were washed and 100 μL/well of dichlorofluorescein diacetate (DCFH-DA) (10 μM) were added. After 1 h of incubation at 37 °C, Caco-2 cells were washed and 100 μL of H_2O_2 0.3 % (v/v) were added to each well. Following 30 min incubation at room temperature, the formation of DCF-DA, the fluorescent oxidised derivative of DCFH-DA, was monitored with a plate reader (SpectraMax® M3, Molecular Devices) (emission and excitation wavelengths of 535 nm and 485 nm, respectively). Fluorescent levels from DCF-DA are directly proportional to intracellular ROS levels (Jiménez et al., 2016).

2.8 Statistical analyses

Statistical analysis was performed using the OriginPro 8.0 software (OriginLab Corp, Buckinghamshire, UK). The normal distribution was assessed by the Shapiro-Wilk normality test. The data was compared using ANOVA test or a Mann-Whitney non-

parametric test. Differences were considered statistically significant at *p< 0.05. The results are expressed as the means ± SD, unless otherwise stated.

3. Results and discussion

Localised delivery of drugs to the intestinal epithelium is a promising therapeutic approach for the treatment of IBD. The rationale is to focalise drugs at the injured tissue site while avoiding the side effects associated to their systemic absorption. We have designed a surfactant-mediated nanoemulsion for CC able to accumulate within the enterocytes and concentrate there its antioxidant capacity.

3.1 Physicochemical characterisation and colloidal stability

The landmark in colloidal drug delivery is the design of stable and efficient nanocarriers for the delivery of molecules to the target tissue while maintaining a low toxicity profile. In this work, we have faced this goal by designing nanoemulsions with just three components formulated by the well-known solvent displacement technique. This procedure allows the formation of nanoemulsions under mild conditions by using hydrophobic excipients. The selection of the materials was carefully carried out, as their nature and disposition would influence the biological behaviour of the system. We have previously described that the hydrophobic nature of the core in nanoemulsions determines the effective adsorption of the surfactants. In this work we selected α-tocopherol due to its high hydrophobicity (M. J. Santander-Ortega et al., 2017). Hydrophobic ascorbic acid derivatives, e.g. palmitate derivatives, are compounds widely used in the pharmaceutical industry and in the formulation of nanocarriers (Higashi et al., 2017; Moribe et al., 2010; Zariwala et al., 2014). Indeed, we have recently shown that these compounds can be used as surfactants for nanoemulsion stabilisation (Plaza-Oliver et al., 2020). Among them, ADP was the most promising molecule and thus it was selected for the formulation of the systems included in this work. More concretely, ADP was incorporated at two different amounts, 9 and 17 mg,

to determine the effect that the amount of ADP has on its targeting ability to the enterocytes. In this line, we have also formulated a nanoemulsion control where the interface was stabilised by lecithin instead of ADP. The emulsifying and dispersing properties of lecithin are well-known and therefore it has been widely used in the formulation of nanosystems (Hu et al., 2012; Nijaporn Yanasarn, Brian R. Sloat, 2009; Plaza-Oliver et al., 2015; M. J. Santander-Ortega et al., 2017). The systems stabilised by ADP and lecithin where respectively named as NE1-ADP, NE2-ADP and NE-L.

One important aspect required by the *in vitro* evaluation of the nanoemulsions was their stability in the media used in the experiments. We observed that the dilution of the uncoated systems in cell culture (DMEM) and transport (HBSS) media led to their aggregation (data not shown). This prompted us to consider the coating of the nanoemulsions with a PEG derivative like PF127®, taking into account the stabilisation properties of this type of polymers (D'souza and Shegokar, 2016; Otsuka et al., 2003; M.J. Santander-Ortega et al., 2017), as well as its potential for enhancing the diffusion across the intestinal mucus (M. J. Santander-Ortega et al., 2017; Yang et al., 2011). We selected a range of PF127® amounts per batch for the coating of the nanoemulsions (1.5-12.5 mg). The physicochemical properties of the obtained formulations are included in Table 1. Briefly, all of them exhibited low polydispersity and size values below 200 nm; showing no differences on size ($p > 0.05$) independently of the surfactant type (L or ADP) or the concentration of ADP. Incorporation of increasing amounts of PF127® was clearly evidenced by the reduction of the superficial charge of the formulations (Santander-Ortega et al., 2006). As shown in Figure S1, 3 mg of PF127® was the lowest surfactant quantity that allowed the colloidal stabilization of the different nanoemulsions in cell media. Thus, it was selected for the final composition of NE-L and NE-ADP, as depicted in table 2.

The long-term stability of the nanoemulsions under storage conditions (4 °C), confirmed that all the formulations remained stable for at least 4 weeks (Figure S.2).

The oral route is characterised by harsh conditions like extreme pH, high salinity or the presence of digestive enzymes that may lead to aggregation or degradation of the nanosystems. Bearing this in mind, we evaluated the stability of the nanoemulsions in plain (non-supplemented) SGF and SIF and normal (enzymes enriched) SGF and SIF. Remarkably, all the formulations remained stable in plain SGF and SIF (Figures 1.A and 1.B solid lines and closed symbols), as well as in digestive enzymes enriched SGF and SIF (Figure 1.A and 1.B dashed lines and opens symbols). In this sense, the adsorption of the hydrophilic surfactant PF127® onto the surface of the nanoemulsions could avoid the interaction of the enzymes by steric stabilisation (Plaza-Oliver et al., 2015). Altogether, these results indicate the suitability of the nanoemulsions for their oral administration.

The encapsulation of CC led to no relevant differences in the size of NE-L or NE1-ADP compared to the unloaded formulations (163 ± 10 nm and 173 ± 20 nm, respectively), but slightly decreased their ζ-potential values (-12.6 ± 1.9 mV and -19.9 ± 2.7 mV, respectively). The selection of highly hydrophobic core components, together with the low CC loading, enabled to achieve 100 % encapsulation efficiency of CC for both NE-L and NE1-ADP. Additionally, the drug was retained in the nanostructure even after its dilution in the culture media, showing no release of CC. This was particularly important as CC was considered not only as a therapeutic molecule but also as a probe to determine the transport of the nanoemulsions across the intestinal barrier.

3.2 In vitro evaluation of the transport of the nanoemulsions across the intestinal barrier

The interaction of ADP-stabilised nanoemulsions with the intestinal barrier was assessed following a dual approach that consisted on the quantification of α-tocopherol and CC as essential components of the nanoemulsions. Initially, we carried out cytotoxicity assays of NE-L, NE1-ADP and NE2-ADP to select a safe nanoemulsion concentration for the following studies. None of the tested nanoemulsions reached IC_{50} levels after 2 h, even at the highest

concentrations, in which they were barely diluted (750-900 µL/mL). This could be explained by the well-stablished safety profiles of the materials selected. In line with the scarce toxicity observed, we selected a nanoemulsion dilution equivalent to an α-tocopherol concentration of 3,800 µg/mL and 50 µg/mL of CC.

3.2.1 Evaluation of the permeation of unloaded nanoemulsions in Caco-2 cells monolayers

Remarkably, α-tocopherol is the only component of the oily core in unloaded nanoemulsions, and one of the main components of the formulation. In this work, we have considered that the amount of α-tocopherol determined in the permeation studies would correlate to the nanoemulsion itself, since we were not indirectly following an encapsulated dye but directly quantifying an essential component of the nanoemulsion. This rationale was also followed for CC, which was totally encapsulated within nanoemulsions and had no release. This approach allowed us to circumvent the use of fluorescent probes that have been traditionally applied for the transport studies of nanocarriers. Fluorescent labelling of nanocarriers may modify their physicochemical properties and when encapsulated, fluorescent dyes may be prematurely released from the nanocarrier (Lozano, M.V.; Santander-Ortega M.J.; Alonso, 2020). In this sense, we followed a labelling-free approach, as we quantified α-tocopherol by HPLC in the basolateral side of the inserts and afterwards calculated α-tocopherol P_{app} value for each nanoemulsion. The results indicated that ADP-stabilised nanoemulsions were barely transported across the Caco-2 cells monolayer, showing low α-tocopherol P_{app} values. Furthermore, we observed that increasing ADP concentration did not induce higher permeation rates, as NE1-ADP α-tocopherol P_{app} was significantly higher ($p<0.001$) compared to that obtained for NE2-ADP ($1.98 \times 10^{-7} \pm 7.05 \times 10^{-8}$ cm/s and $1.35 \times 10^{-7} \pm 5.36 \times 10^{-8}$ cm/s, respectively), despite having half of ADP content. This could be related to an optimal level of ADP that avoids the saturation of the transporters; therefore, the system NE1-ADP was selected for the following experiments. On the other hand, NE-L showed a higher permeation value than ADP-NE (Figure 2A). More

concretely, NE-L showed a α-tocopherol P_{app} of 5.46 x 10^{-6} ± 1.11 x 10^{-6} cm/s, significantly higher ($p < 0.001$) than P_{app} values showed by NE1-ADP and NE2-ADP. This result was in line with the widely accepted permeation-enhancing properties of lecithin, mainly explained by its phospholipid composition, similar to cellular membranes (Chen et al., 2016; Heo et al., 2016). Taken together, these results suggest that NE-ADP are promising formulations to achieve a localised drug delivery at the intestinal level.

3.2.2 Evaluation of the permeation of CC-loaded nanoemulsions in Caco-2 cells monolayers

The characteristics of CC involve poor transport rate across the intestinal barrier, as previously observed by several other authors (Beloqui et al., 2016; Kharat et al., 2017). In this experiment, we have observed this same pattern with the control CC-sus (mean size of 9.46 ± 0.48 μm), detecting no CC in the basolateral compartment after its incubation with Caco-2 cells (Figure 2B). Similarly, CC was not able to reach the basolateral side (<LOD 5 ng/mL) after the treatment of the Caco-2 cells with CC-loaded NE1-ADP, but it was detected within Caco-2 cells (data not shown). These results correlated to the ones obtained for the unloaded nanoemulsions, indicating a possible accumulation of the nanocarriers at the cell monolayer where they would deliver the drug. CC-loaded NE-L exhibited higher CC P_{app} (6.99 x 10^{-6} ± 9.08 x 10^{-8} cm/s), which is in line with the high P_{app} values obtained for α-tocopherol. The mechanism of transport of the nanoemulsions could be endocytosis or transcytosis processes considering the size of the formulation (Table 1) as observed by other authors (Fan et al., 2017; Neves et al., 2016). Indeed, Y. Fan *et al.* demonstrated the endocytosis of a lipid nanoemulsion sized 170 nm by Caco-2 cells (Fan et al., 2017). Similarly, A.R. Neves *et al.* have recently observed that the uptake of different lipid nanoparticles of 180 nm in Caco-2 cells occurs mainly by clathrin-mediated endocytosis (Neves et al., 2016). Nevertheless, we need to perform further mechanistic studies to confirm this hypothesis.

3.2.3 Intracellular uptake in Caco-2 cells

The accumulation of ADP-stabilised nanoemulsions within the monolayers was assessed by CLSM. Therefore, we performed the transport experiments with DiD-loaded nanoemulsions, both ADP and lecithin-stabilised, and studied the location of DiD within Caco-2 cell monolayers by CLSM. The images obtained are included in Figure 3 and indicate clear differences depending on the stabilising surfactant. ADP-stabilised nanoemulsions strongly interact with the cells, showing slight differences between NE1-ADP and NE2-ADP. More concretely, increasing the amount of ADP (table 2) did not entail higher uptake of NE2-ADP (Figure 3). This pattern was also observed when the permeation of α-tocopherol was determined, showing significantly ($p<0.001$) higher P_{app} values for NE1-ADP compared to NE2-ADP (Figure 2A). This may point out that there is an optimum amount of ADP to promote the uptake of the nanoemulsions and avoid the saturation of SVCT1, but further research is required to confirm this. Meanwhile, it was not possible to detect DiD within the cellular monolayer after the NE-L treatment. This indicates that the NE-L were not retained within the Caco-2 cells monolayer. Most probably, this formulation could have been transported to the basolateral compartment during the experiment, an assumption based on the high α-tocopherol and CC P_{app} values observed for the unloaded and CC-loaded NE-L (Figure 2).

3.2.4 Effect of ascorbic acid pre-incubation on the intracellular uptake in Caco-2 cells

In view of CLSM results, we proceeded to determine the potential implication of SVCT1 on the nanoemulsions uptake. In fact, Caco-2 cells express many membrane transporters and receptors also found in enterocytes, including the vitamin B_{12} and epidermal growth factor receptors, glucose transporters and sodium-dependent ascorbic acid transporters like SVCT1 (Artursson et al., 2001; Maulén et al., 2003). The transporter SVCT1 has been identified in the apical membrane of both enterocytes and Caco-2 cells (Maulén et al., 2003; May, 2011); thus, it arises as a potential target for promoting the interaction of nanocarriers with the intestinal epithelium. This has been recently investigated by Luo Q. *et al* with ascorbate-conjugated nanoparticles that followed a SVCT1-mediated uptake process (Luo

et al., 2018). Bearing this in mind, we performed CLSM experiments after the pre-incubation of the Caco-2 cells monolayers with an ascorbic acid solution for 24 h (from day 20 to day 21) at a concentration (100 μM) which is within the SVCT1 saturation range (MacDonald et al., 2002). Pre-incubation of Caco-2 cells with the ascorbic acid solution did not affect the integrity of the monolayer, which was confirmed by TEER measurements.

As Figure 4 shows, the intracellular DiD levels were clearly lower compared to those observed in non-pre-treated monolayers with ascorbic acid. Taken together, these results indicated that SVCT1 could effectively be implicated in the uptake of ADP-stabilised nanoemulsions by Caco-2 cells. The presence of ADP on the surface of NE-ADP could boast their interaction with the intestinal epithelium. However, further research in this regard is still required. Regarding the uptake of NE-L, it was not influenced by the pre-treatment of the cellular Caco-2 monolayers with ascorbic acid, what makes sense bearing in mind that SVCT1 is not related to the uptake of phospholipid-like substrates.

3.3 Inhibition of intracellular ROS

Chronic inflammatory disorders like IBD have an excessive accumulation of oxidant species due to cellular oxidative stress, that play a key role in IBD pathogenesis (Guan and Lan, 2018; Kruidenier et al., 2003; Tian et al., 2017). The administration of antioxidants is considered a promising approach to ameliorate the disease progression; one of the molecules proposed for IBD treatment is CC due to its pleiotropic properties, including antioxidant, anti-inflammatory, antitumor and prebiotic (Burge et al., 2019; Sugimoto et al., 2002). The results obtained from the dichlorofluorescein assay of the formulations were expressed in terms of intracellular ROS levels (%), corresponding the highest value (100 %) to the H_2O_2 control. The molecule CC is an effective antioxidant agent as it was observed by the intracellular ROS levels after CC-sus treatment, decreasing them to 60 ± 18 % (Figure 5).

It is important to highlight that the amount of α-tocopherol used was the same in NE-L and NE-ADP (Table 2). This molecule is one of the most powerful lipophilic antioxidants, so it would contribute to the antioxidant capacity of the NE-ADP and NE-L formulations. Instead of having the same effect, we did observe interesting differences in the ability of α-tocopherol nanoemulsions to scavenge intracellular ROS levels depending on their stabilising surfactant (Figure 5). NE-ADP showed a significant ROS decrease, whereas NE-L did not alter intracellular ROS levels ($p < 0.001$). More concretely, NE1-ADP decreased ROS levels to 34 ± 10 %. This means that NE1-ADP has great potential for encapsulating CC and as an antioxidant platform itself. It is worth to mention that despite the antioxidant capacity of ADP, its concentration in ADP-stabilised nanoemulsions was notably lower compared to α-tocopherol concentration (Table 2). Considering these results, it could be hypothesised that the ROS scavenging ability showed by NE1-ADP could be mainly due to α-tocopherol rather than to ADP. Indeed, the ROS levels obtained for NE2-ADP were not significantly different from those of NE1-ADP (data not shown) despite having double amount of ascorbyl derivative. This seems to point out that the role of ADP in these nanocarriers might be related to its transport-mediated surfactant properties rather than to its antioxidant potential (Plaza-Oliver et al., 2020).

On the other hand, intracellular ROS levels also decreased dramatically when CC was encapsulated in NE1-ADP, showing significant differences with the results obtained for NE-L-CC ($p<0.001$). In fact, this formulation was able to reduce ROS even below basal levels, up to 14 ± 5 % (Figure 5), completely reverting the oxidative stress generated by H_2O_2. Additionally, this result showed that the activity of CC was not modified by the formulation process. The encapsulation of CC in the nanoemulsions allows an increase CC stability and solubility, but also provides an antioxidant synergism between the carrier itself and the encapsulated CC.

4. Conclusion

Overall, this work shows that the composition of nanoemulsions determines their interaction with Caco-2 cells, suggesting different future applications depending on the formulation. Based on these results, NE-L would be efficiently transported across the intestinal barrier. Thus, it seems to be a promising formulation for the systemic delivery of poor water-soluble molecules with low bioavailability. On the other hand, ADP-stabilised nanoemulsions seem to be taken up and retained by the Caco-2 cells. Consequently, low systemic exposure of the encapsulated drug would be expected after the oral administration of the nanoemulsion by focalising the therapeutic effect at the damaged tissue. The ascorbic acid transporter SVCT1 can be a valuable mechanism for the development of new formulations, what requires further research to determine its full potential. Other issues that need to be taken into account are the transporter expression pattern in different IBD processes, especially during advanced stages of the disease as well as the patients' heterogeneity in these disorders.

Acknowledgements

Authors thank the financial support provided by *Diputación de Albacete* and the University of Castilla-La Mancha (UCLM) (projects 01110AB026 and 2019/7223). M. Plaza thanks the financial support given by the UCLM (OE154 and 2018/152504) (Spain). A. Beloqui is a Research Associate of the *Fonds de la Recherche Scientifique-FNRS* (Belgium). Authors also thank Dr. J.R. Marín and Dr. J. Soriano for their great support with confocal microscopy.

References

Anand, P., Kunnumakkara, A.B., Newman, R.A., Aggarwal, B.B., 2007. Bioavailability of curcumin: Problems and promises. Mol. Pharm. 4, 807–818. https://doi.org/10.1021/mp700113r

Arafa, H.M.M., Hemeida, R.A., El-Bahrawy, A.I.M., Hamada, F.M.A., 2009. Prophylactic role of curcumin in dextran sulfate sodium (DSS)-induced ulcerative colitis murine model. Food Chem. Toxicol. 47, 1311–1317. https://doi.org/10.1016/j.fct.2009.03.003

Artursson, P., Palm, K., Luthman, K., 2001. Caco-2 monolayers in experimental and theoretical predictions of drug transport. Adv. Drug Deliv. Rev. 64, 280–289. https://doi.org/10.1016/j.addr.2012.09.005

Beloqui, A., Brayden, D.J., Artursson, P., Préat, V., Des Rieux, A., 2017. A human intestinal M-cell-like model for investigating particle, antigen and microorganism translocation. Nat. Protoc. 12, 1387–1399. https://doi.org/10.1038/nprot.2017.041

Beloqui, A., Coco, R., Memvanga, P.B., Ucakar, B., Des Rieux, A., Préat, V., 2014. PH-sensitive nanoparticles for colonic delivery of curcumin in inflammatory bowel disease. Int. J. Pharm. 473, 203–212. https://doi.org/10.1016/j.ijpharm.2014.07.009

Beloqui, A., Memvanga, P.B., Coco, R., Reimondez-Troitiño, S., Alhouayek, M., Muccioli, G.G., Alonso, M.J., Csaba, N., de la Fuente, M., Préat, V., 2016. A comparative study of curcumin-loaded lipid-based nanocarriers in the treatment of inflammatory bowel disease. Colloids Surfaces B Biointerfaces 143, 327–335. https://doi.org/10.1016/j.colsurfb.2016.03.038

Bernstein, C.N., Fried, M., Krabshuis, J.H., Cohen, H., Eliakim, R., Fedail, S., Gearry, R., Goh, K.L., Hamid, S., Khan, A.G., LeMair, A.W., Malfertheiner, Ouyang, Q., Rey, J.F., Sood, A., Steinwurz, F., Thomsen, O.O., Thomson, A., Watermeyer, G., 2010. World gastroenterology organization practice guidelines for the diagnosis and management of IBD in 2010. Inflamm. Bowel Dis. 16, 112–124. https://doi.org/10.1002/ibd.21048

Bitiren, M., Karakilcik, A.Z., Zerin, M., Ozardalı, I., Selek, S., Nazlıgül, Y., Ozgonul, A., Musa, D., Uzunkoy, A., 2010. Protective effects of selenium and vitamin e combination on experimental colitis in blood plasma and colon of rats. Biol. Trace Elem. Res. 136, 87–

95. https://doi.org/10.1007/s12011-009-8518-3

Burge, K., Gunasekaran, A., Eckert, J., Chaaban, H., 2019. Curcumin and intestinal inflammatory diseases: Molecular mechanisms of protection. Int. J. Mol. Sci. 20. 1-36. https://doi.org/10.3390/ijms20081912

Chen, L.C., Chen, Y.C., Su, C.Y., Wong, W.P., Sheu, M.T., Ho, H.O., 2016. Development and Characterization of Lecithin-based Self-assembling Mixed Polymeric Micellar (saMPMs) Drug Delivery Systems for Curcumin. Sci. Rep. 6, 1–11. https://doi.org/10.1038/srep37122

Cui, J., Yu, B., Zhao, Y., Zhu, W., Li, H., Lou, H., Zhai, G., 2009. Enhancement of oral absorption of curcumin by self-microemulsifying drug delivery systems. Int. J. Pharm. 371, 148–155. https://doi.org/10.1016/j.ijpharm.2008.12.009

D'souza, A.A., Shegokar, R., 2016. Polyethylene glycol (PEG): a versatile polymer for pharmaceutical applications. Expert Opin. Drug Deliv. 13, 1257–1275. https://doi.org/10.1080/17425247.2016.1182485

Djiokeng Paka, G., Doggui, S., Zaghmi, A., Safar, R., Dao, L., Reisch, A., Klymchenko, A., Roullin, V.G., Joubert, O., Ramassamy, C., 2016. Neuronal Uptake and Neuroprotective Properties of Curcumin-Loaded Nanoparticles on SK-N-SH Cell Line: Role of Poly(lactide-co-glycolide) Polymeric Matrix Composition. Mol. Pharm. 13, 391–403. https://doi.org/10.1021/acs.molpharmaceut.5b00611

Du, L., Li, J., Chen, C., Liu, Y., 2014. Nanocarrier: A potential tool for future antioxidant therapy. Free Radic. Res. 48, 1061–1069. https://doi.org/10.3109/10715762.2014.924625

Fan, Y., Zhang, Y., Yokoyama, W., Yi, J., 2017. Endocytosis of corn oil-caseinate emulsions in vitro: Impacts of droplet sizes. Nanomaterials 7 (11) 349. https://doi.org/10.3390/nano7110349

Grimpen, F., Pavli, P., 2010. Advances in the management of inflammatory bowel disease. Intern. Med. J. 40, 258–264. https://doi.org/10.1111/j.1445-5994.2010.02163.x

Guan, G., Lan, S., 2018. Implications of antioxidant systems in inflammatory bowel disease. Biomed Res. Int. 2018. 1-7. https://doi.org/10.1155/2018/1290179

Hanai, H., Iida, T., Takeuchi, K., Watanabe, F., Maruyama, Y., Andoh, A., Tsujikawa, T., Fujiyama, Y., Mitsuyama, K., Sata, M., Yamada, M., Iwaoka, Y., Kanke, K., Hiraishi, H., Hirayama, K., Arai, H., Yoshii, S., Uchijima, M., Nagata, T., Koide, Y., 2006. Curcumin Maintenance Therapy for Ulcerative Colitis: Randomized, Multicenter, Double-Blind, Placebo-Controlled Trial. Clin. Gastroenterol. Hepatol. 4, 1502–1506. https://doi.org/10.1016/j.cgh.2006.08.008

Heo, W., Kim, J.H., Pan, J.H., Kim, Y.J., 2016. Lecithin-Based Nano-emulsification Improves the Bioavailability of Conjugated Linoleic Acid. J. Agric. Food Chem. 64, 1355–1360. https://doi.org/10.1021/acs.jafc.5b05397

Higashi, K., Mibu, F., Saito, K., Limwikrant, W., Yamamoto, K., Moribe, K., 2017. Composition-dependent structural changes and antitumor activity of ASC-DP/DSPE-PEG nanoparticles. Eur. J. Pharm. Sci. 99, 24–31. https://doi.org/10.1016/j.ejps.2016.11.029

Hu, K., Cao, S., Hu, F., Feng, J., 2012. Enhanced oral bioavailability of docetaxel by lecithin nanoparticles: Preparation, in vitro, and in vivo evaluation. Int. J. Nanomedicine 7, 3537–3545. https://doi.org/10.2147/IJN.S32880

Hvas, C.L., Bendix, M., Dige, A., Dahlerup, J.F., Agnholt, J., 2018. Current, experimental, and future treatments in inflammatory bowel disease: a clinical review. Immunopharmacol. Immunotoxicol. 40, 446–460. https://doi.org/10.1080/08923973.2018.1469144

Islam, M.S., Aryasomayajula, A., Selvaganapathy, P.R., 2017. A review on macroscale and

microscale cell lysis methods. Micromachines 8 (3) 83. https://doi.org/10.3390/mi8030083

Jiménez, S., Gascón, S., Luquin, A., Laguna, M., Ancin-Azpilicueta, C., Rodríguez-Yoldi, M.J., 2016. Rosa canina extracts have antiproliferative and antioxidant effects on caco-2 human colon cancer. PLoS One 11, 1–14. https://doi.org/10.1371/journal.pone.0159136

Kharat, M., Du, Z., Zhang, G., McClements, D.J., 2017. Physical and Chemical Stability of Curcumin in Aqueous Solutions and Emulsions: Impact of pH, Temperature, and Molecular Environment. J. Agric. Food Chem. 65, 1525–1532. https://doi.org/10.1021/acs.jafc.6b04815

Kontush, A., Finckh, B., Karten, B., Kohlschütter, A., Beisiegel, U., 1996. Antioxidant and prooxidant activity of α-tocopherol in human plasma and low density lipoprotein. J. Lipid Res. 37, 1436–1448.

Kruidenier, L., Kuiper, I., Lamers, C.B.H.W., Verspaget, H.W., 2003. Intestinal oxidative damage in inflammatory bowel disease: Semi-quantification, localization, and association with mucosal antioxidants. J. Pathol. 201, 28–36. https://doi.org/10.1002/path.1409

Lozano, M.V.; Santander-Ortega M.J.; Alonso, M.J., 2020. Nanotechnology for Oral Drug Delivery.

Lozano, M. V., Lollo, G., Alonso-Nocelo, M., Brea, J., Vidal, A., Torres, D., Alonso, M.J., 2013. Polyarginine nanocapsules: A new platform for intracellular drug delivery. J. Nanoparticle Res. 15. https://doi.org/10.1007/s11051-013-1515-7

Luo, Q., Jiang, M., Kou, L., Zhang, L., Li, G., Yao, Q., Shang, L., Chen, Y., 2018. Ascorbate-conjugated nanoparticles for promoted oral delivery of therapeutic drugs via sodium-dependent vitamin C transporter 1 (SVCT1). Artif. Cells, Nanomedicine Biotechnol.

46, 198–208. https://doi.org/10.1080/21691401.2017.1417864

MacDonald, L., Thumser, A.E., Sharp, P., 2002. Decreased expression of the vitamin C transporter SVCT1 by ascorbic acid in a human intestinal epithelial cell line. Br. J. Nutr. 87, 97–100. https://doi.org/10.1079/bjn2001492

Maulén, N.P., Henríquez, E.A., Kempe, S., Cárcamo, J.G., Schmid-Kotsas, A., Bachem, M., Grünert, A., Bustamante, M.E., Nualart, F., Vera, J.C., 2003. Up-regulation and polarized expression of the sodium-ascorbic acid transporter SVCT1 in post-confluent differentiated CaCo-2 cells. J. Biol. Chem. 278, 9035–9041. https://doi.org/10.1074/jbc.M205119200

May, J.M., 2011. The SLC23 family of ascorbate transporters: Ensuring that you get and keep your daily dose of vitamin C. Br. J. Pharmacol. 164, 1793–1801. https://doi.org/10.1111/j.1476-5381.2011.01350.x

Memvanga, P.B., Coco, R., Préat, V., 2013. An oral malaria therapy: Curcumin-loaded lipid-based drug delivery systems combined with β-arteether. J. Control. Release 172, 904–913. https://doi.org/10.1016/j.jconrel.2013.09.001

Moribe, K., Maruyama, S., Inoue, Y., Suzuki, T., Fukami, T., Tomono, K., Higashi, K., Tozuka, Y., Yamamoto, K., 2010. Ascorbyl dipalmitate/PEG-lipid nanoparticles as a novel carrier for hydrophobic drugs. Int. J. Pharm. 387, 236–243. https://doi.org/10.1016/j.ijpharm.2009.12.007

Neves, A.R., Queiroz, J.F., Costa Lima, S.A., Figueiredo, F., Fernandes, R., Reis, S., 2016. Cellular uptake and transcytosis of lipid-based nanoparticles across the intestinal barrier: Relevance for oral drug delivery. J. Colloid Interface Sci. 463, 258–265. https://doi.org/10.1016/j.jcis.2015.10.057

Nijaporn Yanasarn, Brian R. Sloat, and Z.C., 2009. Nanoparticles Engineered from Lecithin-in-Water Emulsions As A Potential Delivery System for Docetaxel. Int J Pharm. 379,

174–180. https://doi.org/10.1016/j.ijpharm.2009.06.004.Nanoparticles

Otsuka, H., Nagasaki, Y., Kataoka, K., 2003. PEGylated nanoparticles for biological and pharmaceutical applications. Adv. Drug Deliv. Rev. 55, 403–419. https://doi.org/10.1016/S0169-409X(02)00226-0

Plapied, L., Duhem, N., des Rieux, A., Préat, V., 2011. Fate of polymeric nanocarriers for oral drug delivery. Curr. Opin. Colloid Interface Sci. 16, 228–237. https://doi.org/10.1016/j.cocis.2010.12.005

Plaza-Oliver, M., Baranda, J.F.S.D., Rodríguez Robledo, V., Castro-Vázquez, L., Gonzalez-Fuentes, J., Marcos, P., Lozano, M.V., Santander-Ortega, M.J., Arroyo-Jimenez, M.M., 2015. Design of the interface of edible nanoemulsions to modulate the bioaccessibility of neuroprotective antioxidants. Int. J. Pharm. 490. 209-218. https://doi.org/10.1016/j.ijpharm.2015.05.031

Plaza-Oliver, M., Santander-Ortega, M.J., Castro-Vázquez, L., Rodríguez-Robledo, V., González-Fuentes, J., Marcos, P., Lozano, M. V., Arroyo-Jiménez, M.M., 2020. The role of the intestinal-protein corona on the mucodiffusion behaviour of new nanoemulsions stabilised by ascorbyl derivatives. Colloids Surfaces B Biointerfaces 186, 110740. https://doi.org/10.1016/j.colsurfb.2019.110740

Prantera, C., 2013. Glucocorticosteroids in the treatment of inflammatory bowel disease and approaches to minimizing systemic activity. Therap. Adv. Gastroenterol. 6, 137–156. https://doi.org/10.1177/1756283X12473675

Rescigno, M., Urbano, M., Valzasina, B., Francolini, M., Rotta, G., Bonasio, R., Granucci, F., Kraehenbuhl, J.P., Ricciardi-Castagnoli, P., 2001. Dendritic cells express tight junction proteins and penetrate gut epithelial monolayers to sample bacteria. Nat. Immunol. 2, 361–367. https://doi.org/10.1038/86373

Rogler, G., 2010. Gastrointestinal and liver adverse effects of drugs used for treating IBD.

Best Pract. Res. Clin. Gastroenterol. 24, 157–165. https://doi.org/10.1016/j.bpg.2009.10.011

Santander-Ortega, M.J., Jódar-Reyes, A.B., Csaba, N., Bastos-González, D., Ortega-Vinuesa, J.L., 2006. Colloidal stability of Pluronic F68-coated PLGA nanoparticles: A variety of stabilisation mechanisms. J. Colloid Interface Sci. 302, 522–529. https://doi.org/10.1016/j.jcis.2006.07.031

Santander-Ortega, M. J., Plaza-Oliver, M., Rodríguez-Robledo, V., Castro-Vázquez, L., Villaseca-González, N., González-Fuentes, J., Cano, E.L., Marcos, P., Lozano, M. V., Arroyo-Jiménez, M.M., 2017. PEGylated Nanoemulsions for Oral Delivery: Role of the Inner Core on the Final Fate of the Formulation. Langmuir 33, 4269–4279. https://doi.org/10.1021/acs.langmuir.7b00351

Sharma, M., Sharma, S., Wadhwa, J., 2019. Improved uptake and therapeutic intervention of curcumin via designing binary lipid nanoparticulate formulation for oral delivery in inflammatory bowel disorder. Artif. Cells, Nanomedicine Biotechnol. 47, 45–55. https://doi.org/10.1080/21691401.2018.1543191

Siew, L.F., Man, S.M., Newton, J.M., Basit, A.W., 2004. Amylose formulations for drug delivery to the colon: A comparison of two fermentation models to assess colonic targeting performance in vitro. Int. J. Pharm. 273, 129–134. https://doi.org/10.1016/j.ijpharm.2003.12.015

Stallmach, A., Hagel, S., Bruns, T., 2010. Adverse effects of biologics used for treating IBD. Best Pract. Res. Clin. Gastroenterol. 24, 167–182. https://doi.org/10.1016/j.bpg.2010.01.002

Sugimoto, K., Hanai, H., Tozawa, K., Aoshi, T., Uchijima, M., Nagata, T., Koide, Y., 2002. Curcumin prevents and ameliorates trinitrobenzene sulfonic acid-induced colitis in mice. Gastroenterology 123, 1912–1922. https://doi.org/10.1053/gast.2002.37050

Tian, T., Wang, Z., Zhang, J., 2017. Pathomechanisms of Oxidative Stress in Inflammatory Bowel Disease and Potential Antioxidant Therapies. Oxid. Med. Cell. Longev. 2017. 1-18. https://doi.org/10.1155/2017/4535194

Villaseca-González, N., Robledo, V.R., Castro-Vázquez, L., Lozano, M.V., Santander-Ortega, M.J., González-Fuentes, J., Marcos, P., Mar Arroyo-Jiménez, M. Del, 2018. Ultrafast determination of Vitamin E using LC-ESI-MS/MS for preclinical development of new nutraceutical formulations. Bioanalysis 10, 215–227. https://doi.org/10.4155/bio-2017-0095

Xu, Y., Shrestha, N., Préat, V., Beloqui, A., 2020. Overcoming the intestinal barrier: A look into targeting approaches for improved oral drug delivery systems. J. Control. Release 322, 486–508. https://doi.org/10.1016/j.jconrel.2020.04.006

Yang, M., Lai, S.K., Wang, Y.-Y., Zhong, W., Happe, C., Zhang, M., Fu, J., Hanes, J., 2011. Biodegradable nanoparticles composed entirely of safe materials that rapidly penetrate human mucus. Angew. Chem. Int. Ed. Engl. 50, 2597–600. https://doi.org/10.1002/anie.201006849

Yoo, J., Park, C., Yi, G., Lee, D., Koo, H., 2019. Active targeting strategies using biological ligands for nanoparticle drug delivery systems. Cancers (Basel). 11. https://doi.org/10.3390/cancers11050640

Zariwala, M.G., Farnaud, S., Merchant, Z., Somavarapu, S., Renshaw, D., 2014. Ascorbyl palmitate/DSPE-PEG nanocarriers for oral iron delivery: Preparation, characterisation and in vitro evaluation. Colloids Surfaces B Biointerfaces 115, 86–92. https://doi.org/10.1016/j.colsurfb.2013.11.028

Zhang, L., Wang, S., Zhang, M., Sun, J., 2013. Nanocarriers for oral drug delivery. J. Drug Target. 21, 515–527. https://doi.org/10.3109/1061186X.2013.789033

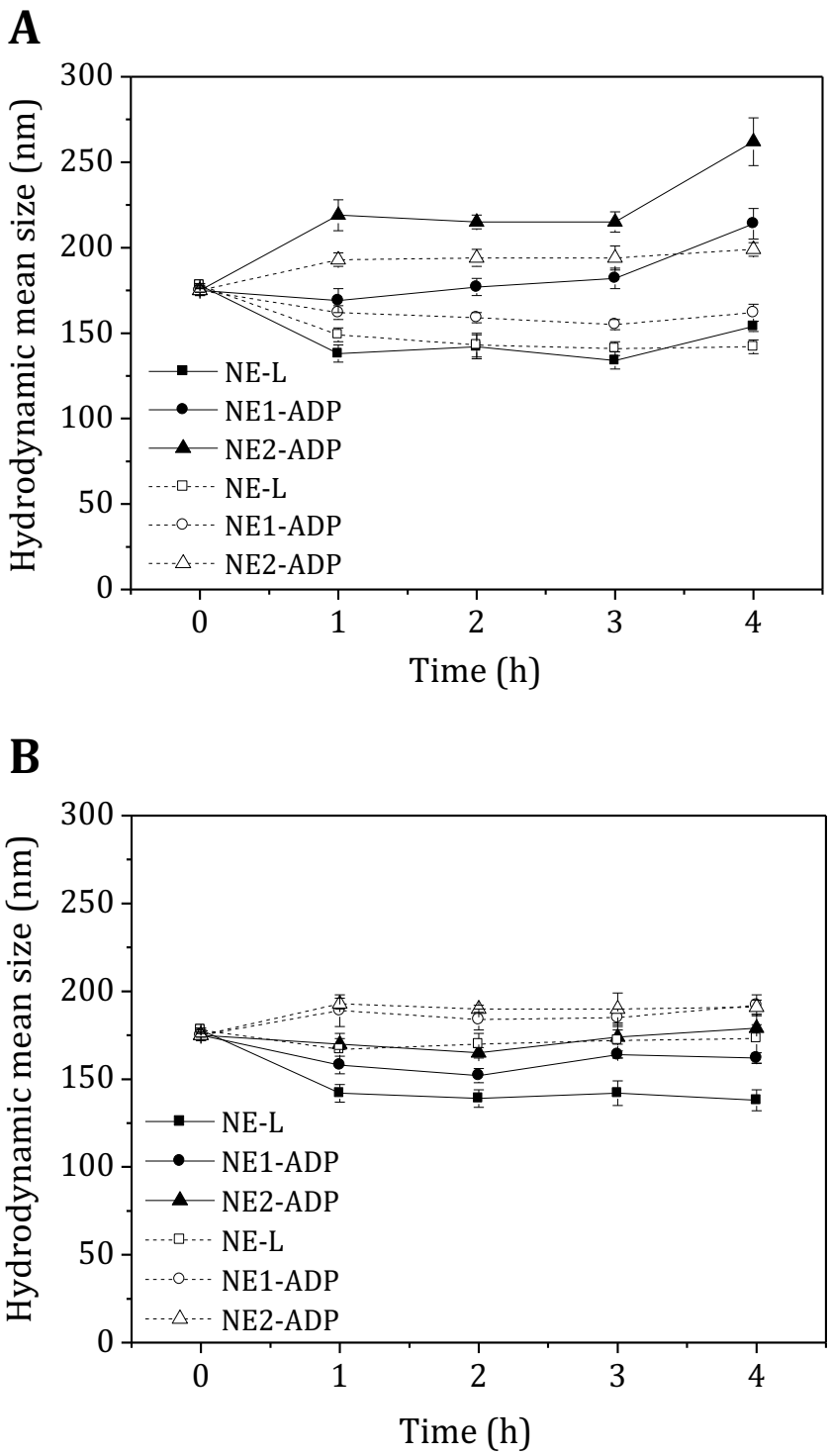

Figure 1 Colloidal stability of lecithin and ADP-stabilised nanoemulsions incubated in (A) non-supplemented SGF (solid line and closed symbols) and in normal SGF (dashed line and open symbols); (B) non-supplemented SIF (solid line and closed symbols) and in normal SIF (dashed line and open symbols) (mean ± SD, n ≥ 3).

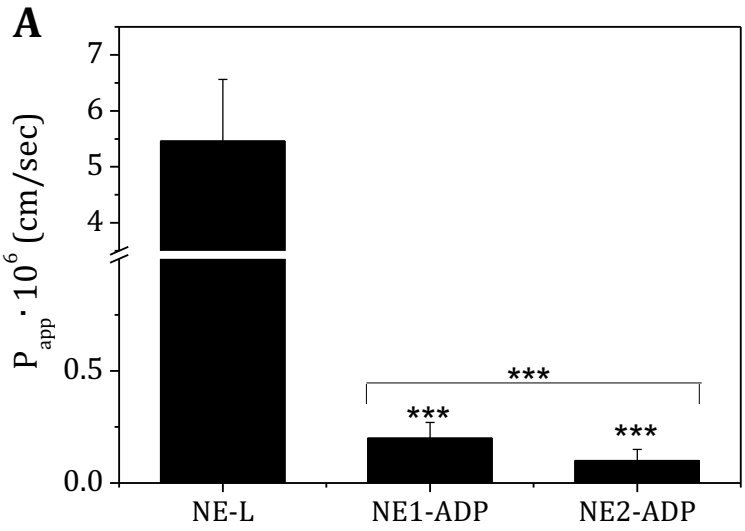

Formulation	$P_{app} \cdot 10^6$ (cm/sec)
NE-L	5.46 ± 1.11
NE1-ADP	0.20 ± 0.07
NE2-ADP	0.10 ± 0.05

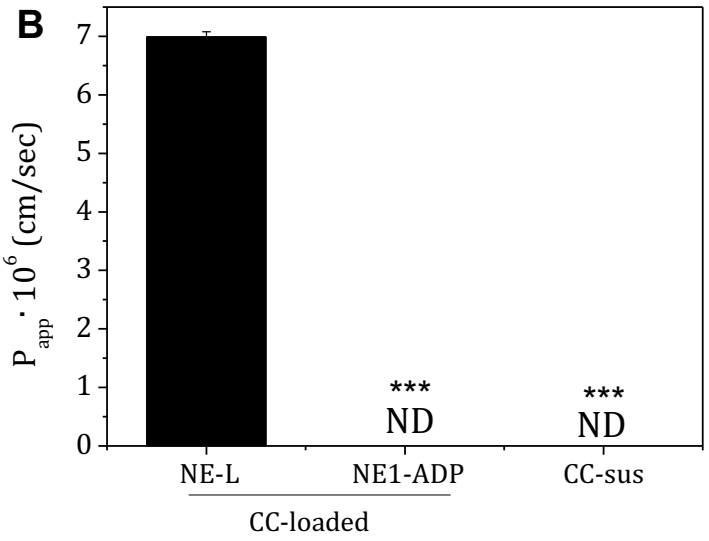

Formulation	$P_{app} \cdot 10^6$ (cm/sec)
CC-loaded NE-L	6.99 ± 0.09
CC-loaded NE1-ADP	ND
CC-sus	ND

Figure 2 Permeability of the nanoemulsions across a Caco-2 cells monolayer. (A) α-tocopherol P_{app} values obtained for NE-L, NE1-ADP and NE2-ADP. (B) CC P_{app} values obtained for CC-loaded NE-L, CC-loaded NE1-ADP and CC-sus. (N=3, n=3, mean ± SEM, ***p<0.001)) (ND: below CC LOD = 5 ng/mL).

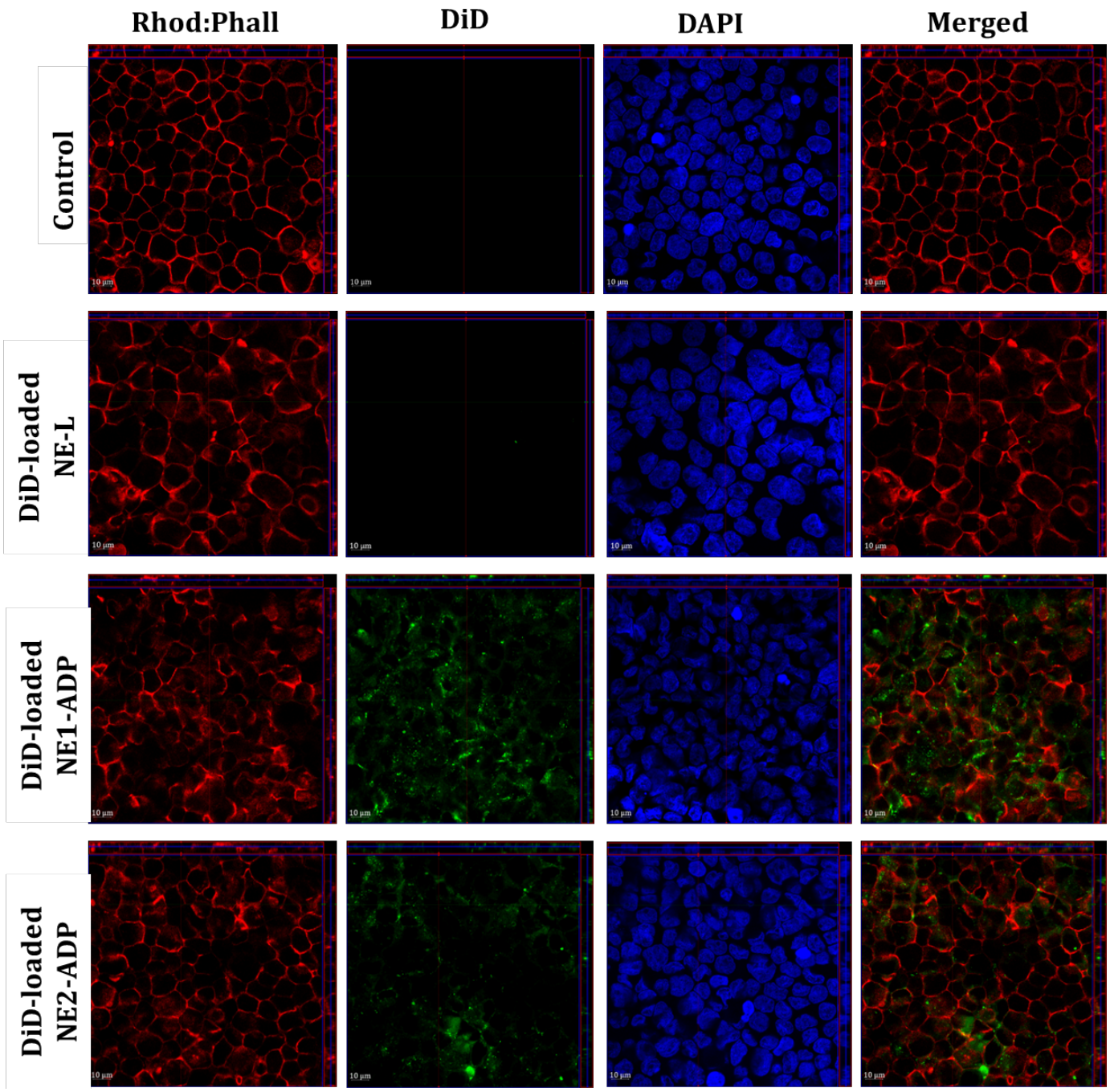

Figure 3 *y-z, x-y* and *x-z* sections of CLSM images of Caco-2 cells monolayers treated with fluorescence-labelled nanoemulsions. DiD appears in green, cell membranes were stained in red with rhodamine-phalloidine and cellular nuclei, stained with DAPI, are shown in blue. For a better visualization, DAPI has not been included in the merged images. For interpretation of the references to colour in this figure legend, the reader is referred to the web version of this article.

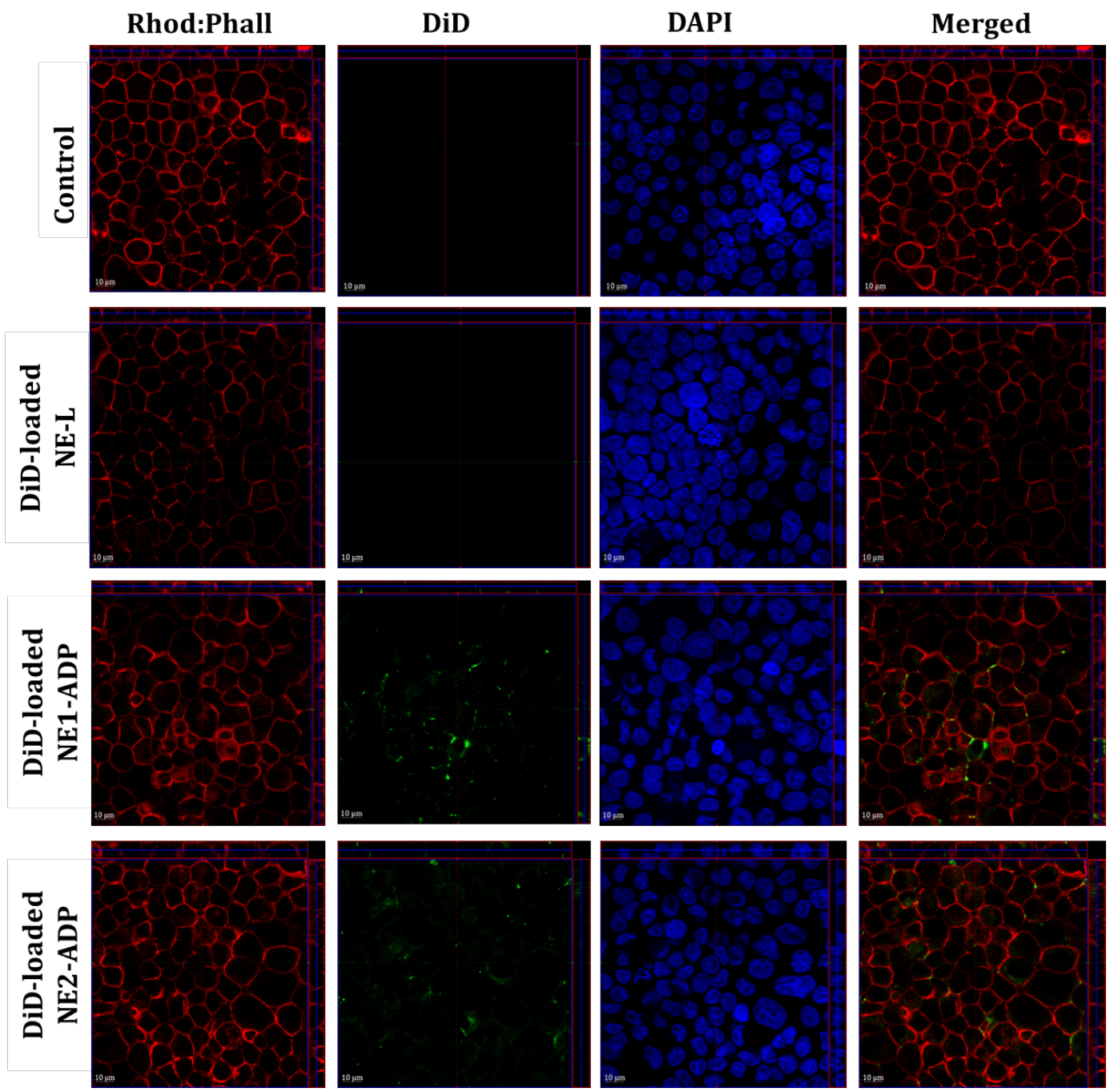

Figure 4 y-z, x-y and x-z sections of CLSM images of Caco-2 cells monolayers after having been pre-treated with ascorbic acid (100 µM) for 24 h and treated with fluorescence-labelled nanoemulsions. DiD appears in green, cell membranes were stained in red with rhodamine-phalloidine and cellular nuclei, stained with DAPI, are shown in blue. For a better visualization, DAPI has not been included in merged images. Comparison with figure 3 helps to observe the effect of ascorbic acid pre-treatment. For interpretation of the references to colour in this figure legend, the reader is referred to the web version of this article.

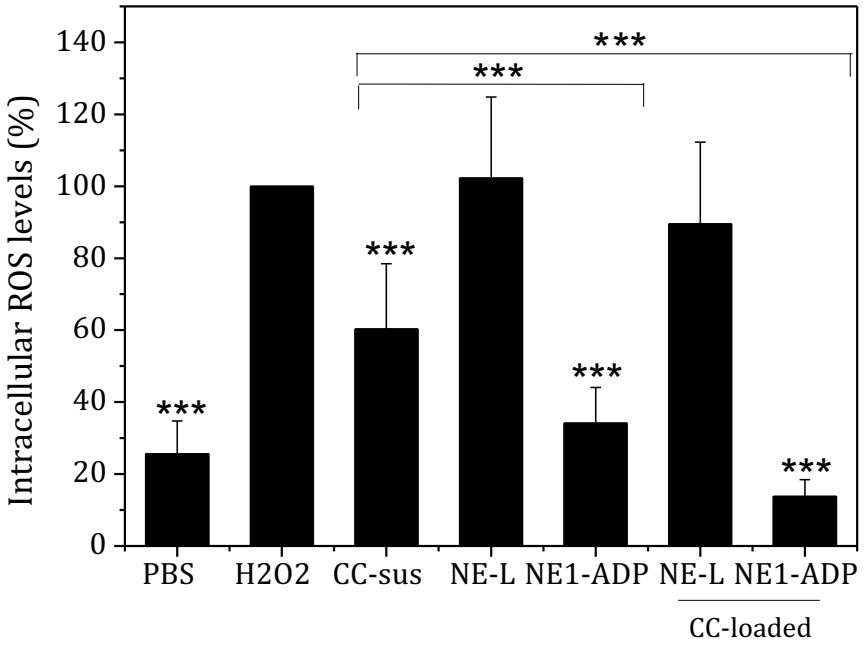

Figure 5 DCFH-DA assay. Effect of CC-sus, unloaded and CC-loaded lecithin and ADP-stabilised nanoemulsions on H_2O_2-induced intracellular ROS generation in Caco-2 cells. (N=4, n=4, mean ± SEM; ***p<0.001).

Table 1. Physicochemical properties of NE-L and NE-ADP coated with different amounts of PF-127® (mean ± SD, n ≥ 3).

Nanoemulsion	PF127® amount (mg)	Hydrodynamic mean size (nm)	PDI	ζ-Potential (mV)
NE-L	0	175 ± 2	0.105	-45.6 ± 3.0
	1.5	180 ± 7	0.126	-35.9 ± 1.7
	3	171 ± 10	0.226	-23.7 ± 4.1
	6	179 ± 4	0.102	-11.6 ± 1.9
	12.5	183 ± 4	0.103	-13.6 ± 1.3
NE1-ADP	0	173 ± 1	0.097	-49.1 ± 2.4
	1.5	172 ± 2	0.120	-39.9 ± 2.5
	3	173 ± 15	0.162	-24.4 ± 2.6
	6	181 ± 3	0.089	-8.7 ± 0.6
	12.5	191 ± 6	0.109	-12.3 ± 1.0
NE2-ADP	0	175 ± 1	0.089	-48.9 ± 3.8
	1.5	172 ± 2	0.093	-35.5 ± 1.4
	3	175 ± 14	0.218	-37.7 ± 1.6
	6	181 ± 1	0.130	-16.2 ± 1.0
	12.5	198 ± 3	0.118	-11.3 ± 0.5

Table 2. Composition of NE-L, NE1-ADP and NE2-ADP.

Components (mg)	NE-L	NE1-ADP	NE2-ADP
α-tocopherol	38	38	38
Soybean lecithin	20	-	-
ADP	-	9	17
PF-127®	3	3	3

A

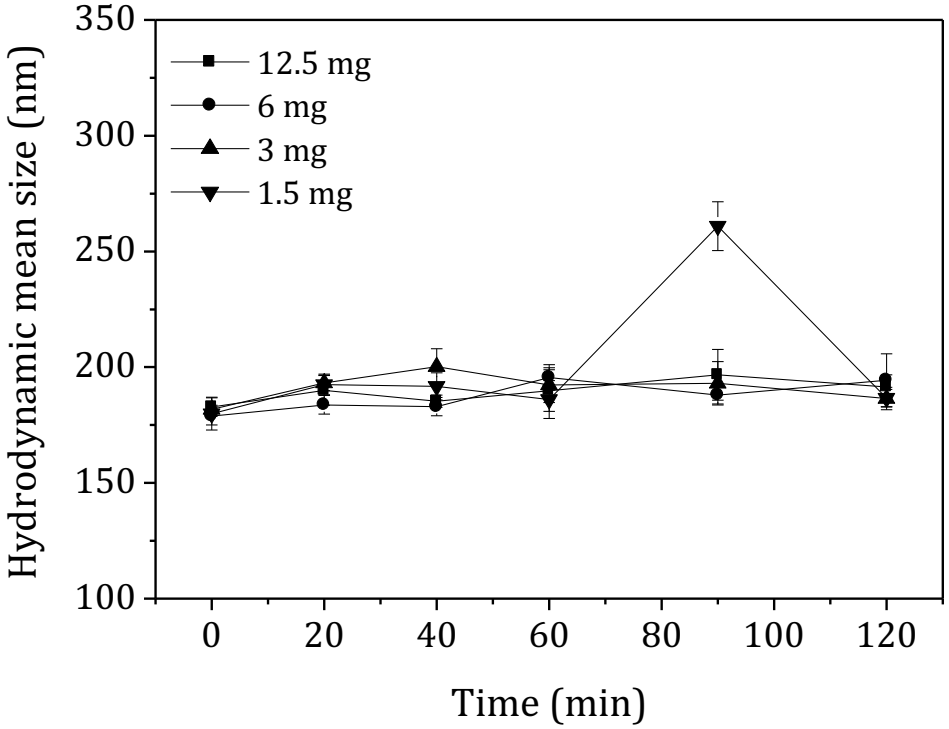
Hydrodynamic mean size (nm)
350
300
250
200
150
100
0
20
40
60
80
100
120
Time (min)
12.5 mg
6 mg
3 mg
1.5 mg

B

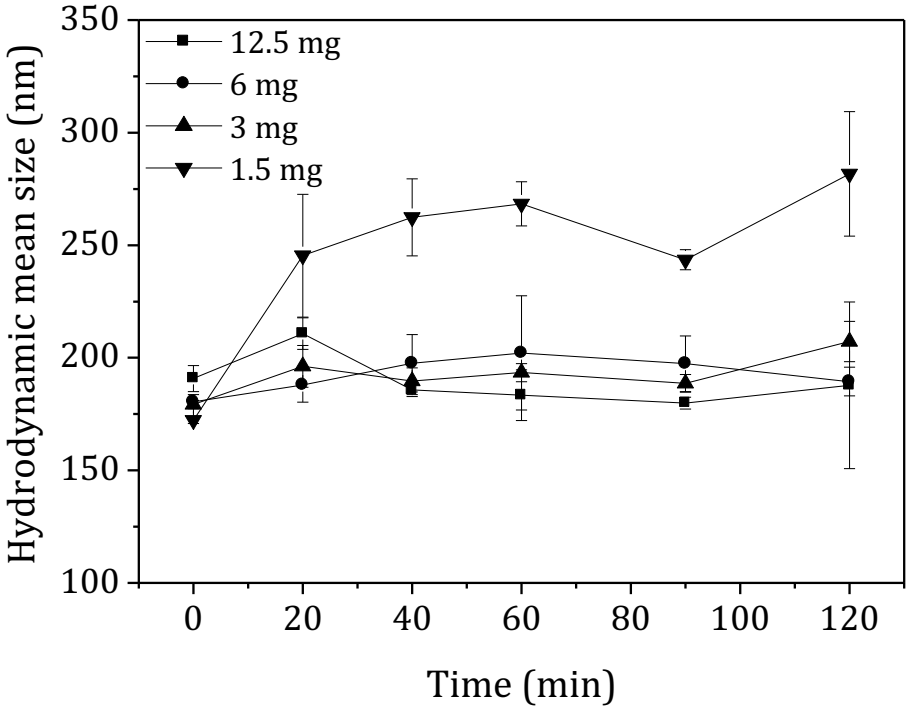
Hydrodynamic mean size (nm)
350
300
250
200
150
100
0
20
40
60
80
100
120
Time (min)
12.5 mg
6 mg
3 mg
1.5 mg

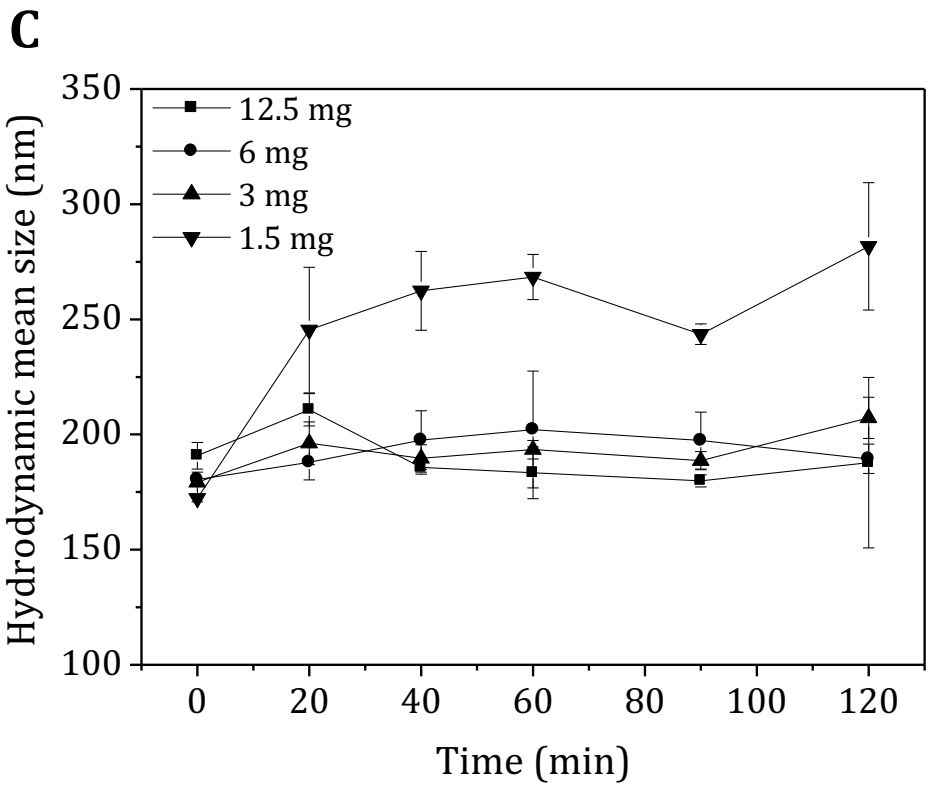

Figure S.1. Colloidal stability of nanoemulsions coated with different amounts of PF127® (12.5, 6, 3 or 1.5 mg) incubated with cell culture grow media (DMEM) at 37 °C for 2 h. (A) NE-L, (B) NE1-ADP, (C)NE2-ADP (mean ± SD, n ≥ 3). The nanoemulsions showed a similar behaviour in the transport media (HBSS) (data not shown).

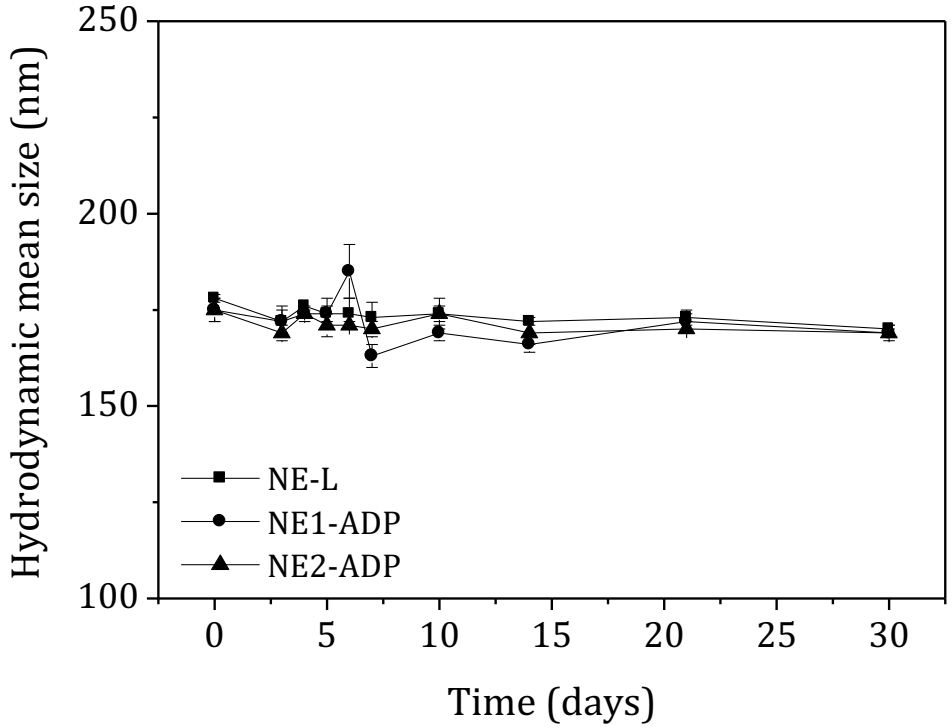

Figure S.2. Long term colloidal stability of lecithin and ADP-stabilised nanoemulsions at 4ºC (mean ± SD, n ≥ 3).